HHS Public Access

Author manuscript

J Biomol Struct Dyn. Author manuscript; available in PMC 2021 October 01.

Published in final edited form as:

J Biomol Struct Dyn. 2020 October ; 38(16): 4921–4927. doi:10.1080/07391102.2019.1688195.

A proposed atomic model of the head-to-tail interaction in the filament structure of vimentin

Raja Dey[a,*], **Peter Burkhard**[b]

[a]The Hormel Institute, Department of Cellular and Molecular Biology, University of Minnesota, 801 16th Ave NE, Austin, MN 55912, USA.

[b]Institute of Materials Science and Department of Molecular and Cell Biology, University of Connecticut, Storrs, CT 06269-3136, USA.

Abstract

The primary building block of all intermediate filaments (IFs) is a coiled-coil dimer, where each monomer consists of a central ?-helical rod domain flanked by an N-terminal head and C-terminal tail domain. Assembly of a class III type IF protein vimentin can be dissected as: (1) formation of tetrameric complexes by two antiparallel, approximately half-staggered coiled-coil dimers (A11 tetramers); (2) rapid lateral association of about eight tetramers into unit-length filaments (ULFs); (3) longitudinal annealing of ULFs into short filaments which further elongate by end-to-end association; and (4) radial compaction of the nascent into mature IFs. We propose and validate an atomic model of the head-to-tail (ACN) interaction of dimers that drives the longitudinal annealing of ULFs and short filaments into nascent IFs. Specifically, we document that a 3-heptad-repeat overlap between the N- and C-terminal ends of coils 1A and 2B yields a stable parallel heterodimeric coiled coil that presumably strengthens the longitudinal annealing process. While circular dichroism enhances the helical content in equimolar mixtures of short coil 1A and coil 2B peptides, isothermal titration calorimetry shows a strong one-on-one interaction between them with a dissociation constant Kd of 3 μM. Dynamic light scattering of an equimolar mixture yields a single species of about 4.7 nm length which comes fairly close to the predicted 5 nm length, while the two peptides individually aggregate. Our newly built computational model elucidates structural detail of ACN interaction within the mature IF and nicely explains, why those IF consensus motifs are so highly conserved.

Keywords

Intermediate filament consensus motif; coiled-coil heterodimer; longitudinal annealing; heptad repeat; hydrophobic interaction

Introduction

Intermediate filaments (IFs) represent one of the three major cytoskeletal filament systems, with IF proteins being found in all metazoan cells including vertebrates, nematodes and

*Correspondence to Raja Dey: rddey80@gmail.com.

molluscs. The other two components of the cytoskeleton, actin containing microfilaments and microtubules, are also found in plants, fungi and protozoa. IF proteins are present in both the cytoplasm and the nucleus, and they are involved in a large number of tissue-specific human diseases related to muscle, heart, skin and neuronal disorders (Eriksson et al., 2009; Omary, 2009). The primary building block of all IFs is a parallel coiled-coil dimer with each monomer consisting of a central α-helical rod domain flanked by an N-terminal head and C-terminal tail domain (Goldie et al., 2007; Sokolova et al., 2006;Strelkov et al., 2004a; Strelkov et al., 2004b; Strelkov et al., 2002). A coiled-coil structure, usually a left-handed super-helix, can be formed by coiling α-helices around each other. Depending on the amino-acid sequence of the α-helices and the biochemical environment, a coiled coil can be a dimer, trimer, tetramer, or pentamer and the helices can be arranged in parallel or anti-parallel fashion. A heptad repeat, defined by the repeating pattern (abcdefg)n, in the primary sequence is an essential criterion for left-handed coiled coils, and the amino acids at the coiled-coil interface in the ‘a’ and ‘d’ positions are usually occupied by hydrophobic residues. The central rod domain consists of two different segments, coil 1 and coil 2, that are joined by a linker, L12 that may or may not be α-helical. In vertebrate cytoplasmic IF proteins the central rod domain is about 310 amino acids long, whereas in invertebrate cytoplasmic and all nuclear IF proteins it is about 350 amino-acids long as these contain an insertion of six additional heptad repeats in coil 1B.

Several groups have shown that the vertebrate cytoplasmic IF assembly pathway starts from the primary dimeric coiled-coil building block and proceeds via distinct tetramer formation followed by their lateral association into unit-length filaments (ULFs). Next, ULFs longitudinally anneal into short filaments which further elongate by end-to-end association; finally, radial compaction of the nascent filaments yields mature IFs. These distinct assembly steps involve four different modes of dimer-dimer interactions: the so called A_{11}, A_{22} and A_{12}, and the head-to-tail or A_{CN} interaction. The A_{11} interaction refers to the antiparallel alignment of the coil 1 segments of two coiled-coil dimers to form a tetramer. On average eight tetramers laterally associate via antiparallel, dimer-dimer interactions to yield ULFs. Longitudinal annealing of ULFs and short nascent filaments requires simultaneously the A_{22} interaction of dimers, i.e. the antiparallel alignment of the coil 2 segments of two adjacent coiled-coil dimers, and the A_{CN} head-to-tail interaction of two consecutive dimers in the direction of the filament.

Both cytoplasmic and nuclear IF proteins contain two conserved motifs, roughly three heptad repeats long each, which are known as IF consensus motifs (IFCMs). These are located at the N-and C-termini of coil 1 and coil 2, respectively (Kapinos et al., 2010). Chemical cross-linking studies have shown that these rod segments are critically important for dimer-dimer interaction in the mature IF. Proteolytic removal of the head and tail domains including these IFCMs does not affect the formation of dimers or tetramers but it prevents the formation of filaments. These two conserved regions also harbor phenotypically critical residues which when mutated yield disease phenotypes (for example, skin blistering diseases in the case of human epidermal keratins.

From the six different types of IF proteins, the type III IF protein vimentin has been studied most extensively and hence is considered a role model for the entire IF protein family.

Although several crystal structures of different smaller fragments of vimentin have been determined (Chernyatina et al., 2012; Meier et al., 2009; Nicolet et al., 2010), atomic detail of the entire protein within the filament is still missing. Recently, Chernyatina et al. modeled the central rod domain of vimentin using multiple crystal structures of different fragments (Chernyatina et al., 2012). In this context, they also proposed an atomic model of the A_{11}-type vimentin rod tetramer.

A vast amount of existing literature documents the critical role of the A_{CN} head-to-tail interaction of consecutive dimers in the direction of the filament to drive the longitudinal annealing of ULFs and short nascent filaments to eventually yield a long mature IF (Isobe et al., 2007). Multiple phosphorylation sites have been identified in the head domain, which play an important role in regulating the assembly and disassembly process of IFs (Eriksson et al., 2004). A recent study on vimentin filament assembly based on hydrogen-deuterium exchange reaction (Premchandar et al., 2016) revealed that the interaction between the coils 1A and 2A belonging to two neighboring tetramers is responsible primarily for lateral association towards ULF formation. They also have shown that four point mutations in this IFCM regions cause an assembly arrest at the ULF stage. In this regard, the authors concluded that a rearrangement of the coil 1A-coil 2A complex of individual dimers is necessary to enable coil 1A/coil 2B interaction for the longitudinal annealing of ULFs with one another. But, there is no structural information of the A_{CN}-type head-to-tail interaction available even half a century after the amino-acid sequence of an IF protein was first determined.

Here, we have analyzed a set of short peptides of the IFCMs of the central α-helical rod domain of human vimentin and built a computational model of the A_{CN} coiled-coil interaction in atomic detail based on our hypothesis that involves a 3-heptad-repeat overlap of coil 1A with coil 2B. Accordingly, the A_{CN} head-to-tail interaction of two consecutive vimentin coiled-coil dimers is a parallel heterodimeric coiled coil formed by the IFCMs of coil 1A and coil 2B (Scheme 1). This model is based on our previous hypothesis of the head-to-tail interaction proposed for nuclear lamin dimers (Kapinos et al., 2011). This heterodimeric A_{CN} coiled-coil interaction is supported by a number of biophysical data, including circular dichroism, isothermal titration calorimetry and dynamic light scattering. Taken together, our newly built computational model of the A_{CN} head-to-tail interaction elucidates structural detail of the longitudinal dimer-dimer interaction within the mature IF and nicely explains why those IF consensus motifs (IFCMs) are so highly conserve

Materials and Methods

Peptides

The six peptides (Fig. 1) were synthesized by Biomatik, Wilmington, DE. Details of the rationale behind the 6 peptides designed are described in the Results and Discussion section 3.2. All peptides were dissolved in 10 mM Tris (pH8.0) at a concentration of around 0.3mg/ml. Concentration was measured using the UV absorption calculated at 280 Å with a NanoDrop-2000 spectrophotometer.

Circular dichroism

Circular dichroism (CD) spectrum analysis was performed with a Pi-Star 180 circular dichroism spectropolarimeter. The temperature was maintained at 20°C with a circulating water bath and a path-length of 0.1-cm was used for CD wavelength scans. Wavelength scans were done over the range of 190–250 nm and sampled every 1 nm with a band width of 2 nm and a scan time of 30 minutes.

Isothermal calorimetry

We performed the ITC experiment with peptides 91a and 374a using a NANO ITC, low volume (TA Instruments, New Castle, DE), where peptide 374a at a concentration of 0.540mM was injected into the cell containing peptide 91a at a concentration of 0.095mM. 50μl of peptide 374a was injected into the cell containing 350μl of peptide 91a by 20 injections each of 2.5μl. The raw heat rate reached saturation after 1 hour 30 min.

Dynamic light scattering

The hydrodynamic diameter was determined with a Malvern Zetasizer Nano S equipped with a 633 nm laser using a 3 mm path length quartz suprasil cell. The measurements were performed at 25°C using 60 μl samples at a concentration of 1 mg/ml and for each peptide five scans were collected and the average was recorded. The volume-average hydrodynamic sizes were calculated using the Malvern DTS software, version 6.01. Peptides 91a and 374a were both dissolved in 10mM Tris (pH 8.0) followed by dialysis against a denaturing buffer containing 10mM Tris (pH 7.5), 4M urea, and 50mM NaCl. The concentrations were measured using the NanoDrop-2000 spectrophotometer. To prepare the final sample an equimolar mixture of denatured peptides 91a and 374a was then sequentially dialyzed with 4M, 2M, and 0M urea containing buffer (10 mM Tris at pH 7.5, 50mM NaCl).

Results and Discussion

Atomic model of a parallel heterodimer between coils 1A and 2B at the opposite ends of coiled-coil rod domain of vimentin

We have investigated the possible arrangements of the A_{CN} interaction within the mature filament. Assuming a direct interaction of the N-terminal and C-terminal IFCMs segments with each other in the A_{CN} interaction there are essentially the following six possibilities of overlap between two coiled coils: these segments can form (i) two parallel homodimers, (ii) two antiparallel homodimers, (iii) two parallel heterodimers, (iv) two antiparallel heterodimers, (v) a parallel heterotetramer, and (vi) an antiparallel heterotetramer. The antiparallel arrangements would imply a head-to-head and a tail-to-tail interaction and hence can most likely be excluded based on previously published cross-linking data.

Given the fact that the long segments of coil 1 and coil 2 are homodimeric coiled coils, the first option (two parallel homodimers) seems to be the obvious choice. However, there is growing evidence that this most obvious arrangement does not reflect the real situation. Interestingly, quite a while ago we have shown that the crystal structure of coil 1A – corresponding essentially to the N-terminal IFCM – is a monomeric α-helix (Strelkov et al., 2002), hence the IFCM of coil 1A is certainly not a very stable homodimeric coiled coil – if

at all. Later we have shown that forcing the coil 1A into a stable dimeric coiled coil in fact abrogates filament formation and stalls the assembly process at the ULF-stage (Meier et al., 2009). Hence, a stable parallel homodimeric coiled coil through IFCM of coil 1A appears to be not compatible with longitudinal annealing of the filament and therefore is a rather unlikely structure of coil 1A in the context of the A_{CN} interaction (Chernyatina et al., 2012).

But also more recent crystal structures of the coil 2 of vimentin (pdb ID 1GK4) and lamin (pdb ID 2XV5) surprisingly showed that the IFCM of coil 2 by no means is an obligate parallel homodimeric coiled coil either, and quite a few alternate coiled-coil arrangements have been found (Kapinos et al., 2011; Nicolet et al., 2010) (see also Fig. 2). We then reasoned that the A_{CN} interaction might be formed by two parallel heterodimers, or a parallel heterotetramer (Kapinos et al., 2010). Here we present more supporting data for a model in which the A_{CN} interaction is formed by two parallel heterodimers using molecular modeling and biophysical analyses.

To study the A_{CN} interaction, we analyzed two different sequence alignments between the IFCM of coil 1A and coil 2B of vimentin, respectively. In Fig. 3, panel a) depicts a three heptad repeat overlap between coil 1A and coil 2B, while panel b) shows a two heptad repeat overlap between these two IFCMs. A stable coiled-coil conformation can be established by face-to-face registering of hydrophobic core residues from adjacent helices. Likewise a destabilization will occur if charged residues occupy these positions. The core positions ‘a’ and ‘d’ of the heptad repeat motif have to be mainly hydrophobic to form a coiled-coil dimer. Thus, a coiled-coil homodimer formed by coil 1A would be unfavorable as the two charged residues R100 and E103 at core positions ‘a’ and ‘d’ would face each other (shown in red color in the amino-acid sequence of coil 1A – Fig. 3a). Similarly, in the amino-acid sequence of coil 2B, the two core residues K390 and E407 (shown in red color) would also be unfavorable for the formation of a coiled-coil homodimer of coil 2B (Fig. 3a). Therefore, these red colored residues in the core positions are expected to destabilize the formation of the homodimeric coiled-coil within coil 1A and also within coil 2B. This would explain the results of the crystallographic studies (Chernyatina et al., 2012; Meier et al., 2009; Strelkov et al., 2002) that shows that these IFCMs do not assume a parallel homodimeric coiled-coil conformation.

In the alignment with a two heptad repeat overlap between coil 1A and coil 2B unfavorable core residues R100 and K390 with the same positive charge are found to be in register and thus to be face to face with each other (Fig. 3b). These residues would repel each other making such a heterodimeric overlap unstable and therefore rather unlikely. However, things look significantly different in the hetreodimeric coiled-coil arrangement with a three heptad repeat overlap (Fig. 3a). Thus we hypothesize that the three heptad repeat overlap is more favorable than the two heptad repeat overlap for the formation of a parallel heterodimeric coiled coil between the IFCMs.

As mentioned above, the crystal structure of the lamin A fragment (residues 328–398, PDB code 2XV5), which harbors a short segment of the tail domain, showed that coil 2B forms an antiparallel coiled-coil conformation (Kapinos et al., 2011). In this crystal structure two different antiparallel interfaces have been observed. One is the right-handed side-by-side

antiparallel interaction. The other - a left-handed, staggered antiparallel interaction between coil 2B of lamin A - may serve as a model template for the A_{CN} interaction (Kapinos et al., 2011). We propose that this staggered conformation of coil 2B in lamin A mimics the spatial arrangement of coils 1A and 2B in our model of the heterodimeric A_{CN} interaction. Thus, one helix corresponds to coil 2B and the other resembles coil 1A as a parallel heterodimer in such a model of the A_{CN} interaction (Fig. 2b). In this figure the antiparallel staggered coiled-coil dimer of lamin A, the guiding mimicry (H1 in blue), has been paired with the symmetry related copy (H2') of the other helix H2 (red) in the asymmetric unit (Fig. 2a). We superposed residues L380 – E405 of one helix of the parallel coiled-coil homodimer of vimentin coil 2B (PDB code 1GK4 - orange) on residues L356 – E381 of one helix (H1) of lamin A, the guiding mimicry mentioned above. The other helix of the coil 2B homodimer automatically follows the helix (H2') of the lamin antiparallel coiled-coil staggered homodimer (Fig. 2b). This structural analysis of the staggered antiparallel coiled-coil conformation of lamin A supports the model of a parallel heterodimeric coiled-coil (A_{CN}) interaction. Now residues E103 – R122 of the unzipped homodimer of coil 1A of vimentin (PDB code 3S4R) are superposed onto residues L386 – E405 of vimentin coil 2B (Fig. 2b). This superposition results in the atomic model of the parallel heterodimeric coiled coil interaction between the two IFCMs of vimentin characterized by a three heptad repeat overlap (Fig. 3a & Fig. 4). Both superposition and model building were done using Pymol.

The three-dimensional atomic structure of this heterodimer with the three heptad repeat overlap is shown in Fig. 4. Coils 1A and 2B of vimentin are shown in green and orange, respectively. In Fig. 4a, E103 of coil 1A from the upper helix (green) is forming charged and H-bonding interactions with K390 and Y383 of the partnering helix of coil 2B below (orange). These interactions are also depicted in the sequence alignment below the diagram. K390 of coil 2B (orange) is forming two charged and H-bonding interactions with E103, E106 and N102 of the heterodimeric coiled-coil partner of coil 1A (green – see also Fig. 4a and Table 1).

From the other side of this model, R100 of coil 1A is forming charged and H-bonding interactions with E382 and H379 of the partner helix of coil 2B (Fig. 4b). In Fig. 3c, L107 and L110 of coil 1A from the upper helix are making strong hydrophobic interactions with the neighboring residues L386, V389, and L393 of the heterodimeric coiled-coil partner of coil 2B as can also be seen in the sequence alignment below the diagram. Thus, the strong hydrophobic interaction on one side of the interface along with several salt-bridge interactions on both sides make this a very plausible model of a parallel heterodimer between the two IFCMs of vimentin. A summary of all these interactions is shown in Table 1.

Designing short peptides at the N and C termini of the central rod domain of vimentin

To validate this model by experimental observations we synthesized two sets of peptides with exactly the same sequence as the IFCMs. However, short peptides lacking the context of the fully assembled filament are unlikely to display detectable biophysical properties of heterodimer formation, even if they have exactly the same sequence as the wild-type. Therefore, one set of peptides (peptides 91a and 374a) was optimized with respect to

heterodimer formation, while the other pair of peptides (peptides 91b and 374b) was optimized for α-helical stability only (Fig. 1). All modifications are located at the end of the peptides while keeping the conserved portions of the consensus sequences exactly as in the wild-type.

For the first pair of peptides (91a and 374a) the following modifications were made: to strengthen the hydrophobic interaction between the two helices we changed asparagine 93 and phenylalanine 96 of peptide 91a and methionine 376 and histidine 379 of peptide 374a into leucine residues. These residues are located in the 'a' and 'd' positions of the first heptad of the two peptides. At the C-terminal end only a very subtle change of valine 121 to leucine has been made in peptide 91a, while the change of glutamate 407 of peptide 374a to leucine is more substantial. To introduce an additional stabilizing g to e' inter-helical salt-bridge between the two peptides, we mutated leucine 380 to glutamate in the first heptad repeat of peptide 374a (Fig. 1). For favorable interaction with the helix dipole and for balancing the overall charge of the peptides, we have introduced both positive and negative charges in the peptides. At the N-terminus of peptide 91a, alanine 91 was replaced with glutamate while isoleucine 92 was changed to an arginine and at the C-terminus glutamines 126 and 127 were changed to arginines. These changes will stabilize the monomeric α-helices. As a result the overall charge changes from −1 to +3 in peptide 91a, and thus compensates the overall charge −3 of peptide 374a. Finally, to further increase the α-helicity of the peptides the two residues threonine 94 and glycine 406 were mutated to alanine in peptide 91a and 374a, respectively.

Since these modifications will bias the model towards the formation of a parallel heterodimeric coiled coil, we designed two more peptides (peptides 91b and 374b) with alanine mutations at both ends of the peptides flanking the conserved IFCMs (Fig. 1). The peptides 91b and 374b will thus be stabilized with respect to monomeric α-helicity only, and coiled-coil formation between peptides 91b and 374b would mainly be attributed to the wild-type interactions between coil1A and 2B.

The biophysical properties of these peptides were then analyzed by circular dichroism (CD), isothermal calorimetry (ITC) and dynamic light scattering (DLS)

Circular dichroism experiment

The CD experiments were performed with two pairs of peptides. All peptides were analyzed individually and then also after co-assembly of peptide 374a with either peptide 91a or peptide 91b. Because peptide 374b was insoluble it could not be included in the CD analysis. Fig. 5a shows that peptide 91a alone displays significant random coil conformation with a low helical percentage, whereas, peptide 374a on its own is showing about 50% helical content. When the two peptides are mixed at equal concentrations, the CD spectrum shows that the minimum at 222 Å is more pronounced compared to the minimum observed in peptide 374a alone (Fig. 5a). The CD spectrum of a biological sample containing a helical secondary structure is characterized by two minima at 208 Å and 222 Å. The minima at 222 Å should be more pronounced if the helical content increases in the sample. The increase of the helical content clearly indicates that peptides 91a and 374a form a coiled coil upon mixing. The CD spectrum for this mixture shows about 65% helicity, indicating a stable

coiled-coil formation between them. Also when peptide 91b is mixed with peptide 374a, the helical content increases from about 50% to 60% in the equimolar mixture, thus indicating the formation of a coiled-coil conformation between them (Fig. 5b). Thus, even the alanine-mutant peptide 91b that lacks the stabilizing modification for heterodimer formation most likely forms a coiled-coil heterodimer with the peptide 374a. This observation supports our model of the head-to-tail interaction as a heterodimeric coiled coil between the two IFCMs.

Isothermal calorimetry experiment

In addition to CD spectroscopy analysis, we have also performed ITC experiments between peptides 91a and 374a to understand their binding thermodynamics. Wild type peptides 91wt and 374wt of coil 1A and coil 2B (Figure 1) were also studied by ITC experiments. The ITC experiment with peptides 91a and 374a showed an enthalpy-driven interaction (Fig. 6) with a dissociation equilibrium constant K_d of 3 μM and a stoichiometric ratio n close to 1. While these thermodynamic parameters demonstrate a strong interaction between peptides 91a and 374a, ITC experiments with either peptide 91b or peptide 91wt in the injection syringe as titrants and 374wt as titrant in the cell showed only very weak interactions between the peptides (data not shown).

Dynamic light scattering experiments

Two peptides with equal volume and molar concentration were mixed in denaturing conditions after dialysis into urea containing buffer. The peptides of this mixture were then refolded by step-wise dialysis with decreasing concentration of urea (4M, 2M, and 0M) to prepare the final sample for the DLS experiment. 50mM NaCl and 10mM Tris-HCl (pH 7.5) have been used as final buffer for the dialysis. The size distribution by volume of the mixture of the two peptides results in a single peak at 4.7nm, which is close to the theoretically predicted molecular size of a heterodimeric coiled coil of about 5nm (Fig. 7). The individual fragments dialized to the same buffer conditions gives larger molecular sizes with DLS peaks at about 900 nm and 540 nm for peptides 91a and 374a, respectively. This observation indicates that aggregation is occurring for the peptides 91a and 374a on their own, whereas in an equimolar mixture they are forming a structure of the size that would be expected for a heterodimeric coiled coil.

Conclusion

The so-called A_{CN} or head-to-tail interaction is an integral part of the longitudinal annealing process during the formation of intermediate filaments. Here we have built an atomic model of this interaction based on the crystal structures of vimentin coils 1A (PDB code 3S4R) and 2B (PDB code 1GK4) homodimers. According to the existing literature, 16 coiled-coil dimers laterally assemble to form a unit length filament of vimentin. When two ULFs anneal longitudinally in head-to-tail fashion, both N and C-termini of coils 1A and 2B, respectively, come in close proximity and according to our model the homodimer is unzipped followed by the formation of 16 heterodimeric coiled coils at the A_{CN} interface. Although one single heterodimeric interaction between the IFCMs of coils 1A and 2B alone contributes only a small binding energy, 16 such heterodimeric coiled-coil interactions (in concert with the other interactions) co-operatively constitute a considerable driving force to anneal ULFs

longitudinally and to create a long mature filament in course of time. A direct interaction of the highly conserved sequences of IF proteins explains their importance for filament assembly and nicely explains, why those IFCMs are so highly conserved.

Acknowledgements

We thank Dr. Ueli Aebi for careful review of the manuscript. This work was supported by NIH Grant 1P01GM096971. The research meets all applicable standards for the ethics of experimentation and research integrity and the article adheres to appropriate reporting guidelines and community standards for data availability. The authors declare no competing financial interest.

References

Chernyatina AA, Nicolet S, Aebi U, Herrmann H, Strelkov SV, 2012 Atomic structure of the vimentin central alpha-helical domain and its implications for intermediate filament assembly. Proceedings of the National Academy of Sciences of the United States of America 109, 13620–13625. [PubMed: 22869704]

Eriksson JE, He T, Trejo-Skalli AV, Harmala-Brasken AS, Hellman J, Chou YH, Goldman RD, 2004 Specific in vivo phosphorylation sites determine the assembly dynamics of vimentin intermediate filaments. J Cell Sci 117, 919–932. [PubMed: 14762106]

Eriksson JE, Dechat T, Grin B, Helfand B, Mendez M, Pallari HM, Goldman RD, 2009 Introducing intermediate filaments: from discovery to disease. The Journal of clinical investigation 119, 1763–1771. [PubMed: 19587451]

Goldie KN, Wedig T, Mitra AK, Aebi U, Herrmann H, Hoenger A, 2007 Dissecting the 3-D structure of vimentin intermediate filaments by cryo-electron tomography. J Struct Biol 158, 378–385. [PubMed: 17289402]

Isobe K, Gohara R, Ueda T, Takasaki Y, Ando S, 2007 The last twenty residues in the head domain of mouse lamin A contain important structural elements for formation of head-to-tail polymers in vitro. Bioscience, biotechnology, and biochemistry 71, 1252–1259.

Kapinos LE, Burkhard P, Herrmann H, Aebi U, Strelkov SV, 2011 Simultaneous formation of right- and left-handed anti-parallel coiled-coil interfaces by a coil2 fragment of human lamin A. J Mol Biol 408, 135–146. [PubMed: 21354179]

Kapinos LE, Schumacher J, Mucke N, Machaidze G, Burkhard P, Aebi U, Strelkov SV, Herrmann H, 2010 Characterization of the head-to-tail overlap complexes formed by human lamin A, B1 and B2 “half-minilamin” dimers. J Mol Biol 396, 719–731. [PubMed: 20004208]

Meier M, Padilla GP, Herrmann H, Wedig T, Hergt M, Patel TR, Stetefeld J, Aebi U, Burkhard P, 2009 Vimentin coil 1A-A molecular switch involved in the initiation of filament elongation. J Mol Biol 390, 245–261. [PubMed: 19422834]

Nicolet S, Herrmann H, Aebi U, Strelkov SV, 2010 Atomic structure of vimentin coil 2. J Struct Biol 170, 369–376. [PubMed: 20176112]

Omary MB, 2009 “IF-pathies”: a broad spectrum of intermediate filament-associated diseases. The Journal of clinical investigation 119, 1756–1762. [PubMed: 19587450]

Aiswarya P, Norbert M, Jarosław P, Tatjana W, Magdalena K-D, Harald H, Michał D, 2016 Structural Dynamics of the Vimentin Coiled-coil Contact Regions Involved in Filament Assembly as Revealed by Hydrogen-Deuterium Exchange. J Biol Chem 291, 24931–24950. [PubMed: 27694444]

Sokolova AV, Kreplak L, Wedig T, Mucke N, Svergun DI, Herrmann H, Aebi U, Strelkov SV, 2006 Monitoring intermediate filament assembly by small-angle x-ray scattering reveals the molecular architecture of assembly intermediates. Proceedings of the National Academy of Sciences of the United States of America 103, 16206–16211. [PubMed: 17050693]

Strelkov SV, Kreplak L, Herrmann H, Aebi U, 2004a Intermediate filament protein structure determination. Methods in cell biology 78, 25–43. [PubMed: 15646614]

Strelkov SV, Schumacher J, Burkhard P, Aebi U, Herrmann H, 2004b Crystal structure of the human lamin A coil 2B dimer: implications for the head-to-tail association of nuclear lamins. J Mol Biol 343, 1067–1080. [PubMed: 15476822]

Strelkov SV, Herrmann H, Geisler N, Wedig T, Zimbelmann R, Aebi U, Burkhard P, 2002 Conserved segments 1A and 2B of the intermediate filament dimer: their atomic structures and role in filament assembly. EMBO J 21, 1255–1266. [PubMed: 11889032]

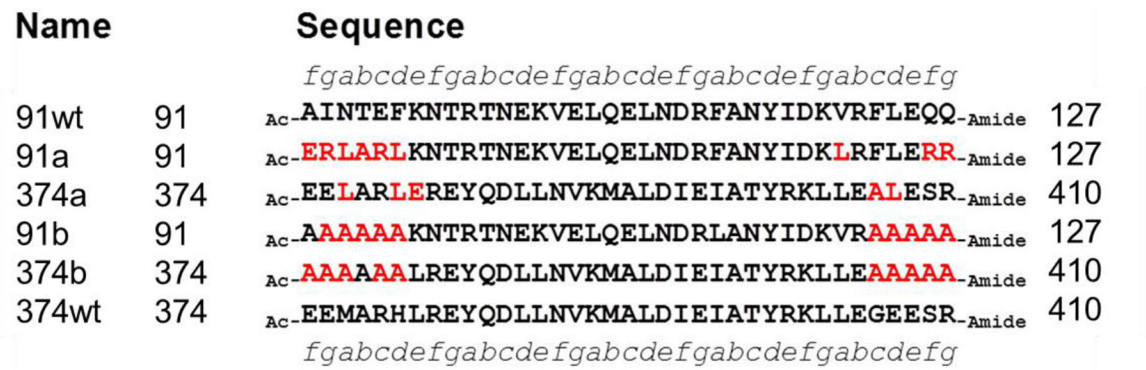

Fig. 1. Sequences of the peptides from coils 1A and 2B of vimentin, respectively.

Peptides 91a and 91b are derived from coil 1A while peptides 374a and 374b are derived from coil 2B of vimentin. Mutations are shown in red. 91wt and 374wt are referred to wild type peptides

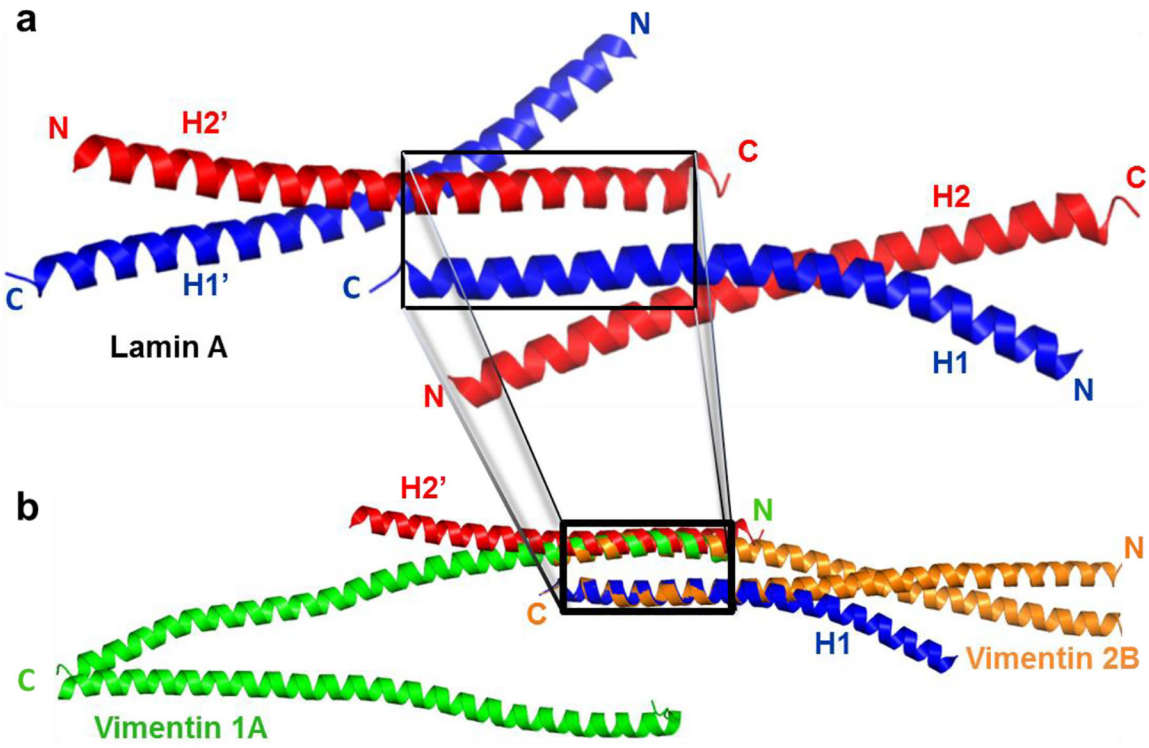

Fig. 2. Three dimensional model building of a parallel heterodimeric coiled coil between coils 1A and 2B of vimentin.

(a) Cartoon diagram of the lamin A fragment (residues 328–398, PDB code 2XV5), with the coiled-coil dimer formed by helices H1 and H2 in blue and red, respectively. Helix H1 also forms a staggered antiparallel heterodimeric coiled-coil with H2', the symmetry related copy of H2 (boxed). (b) One helix of the parallel coiled-coil homodimer of vimentin coil 2B (PDB code 1GK4 - orange) is superposed on helix H1 of lamin (blue), while the other helix of vimentin coil 2B follows the backbone of helix H2' of lamin (red), but in opposite direction. One helix of the unzipped homodimer of the coil 1A fragment of vimentin (PDB code 3S4R - green) is then superposed on this second helix of the vimentin 2B dimer to yield the heterodimeric coiled-coil between the two IFMCs of vimentin (orange and green in the box). Pymol (DeLano Scientific, San Francisco, CA) has been used to build the heterodimeric model of vimentin coils 1A and 2B fragments.

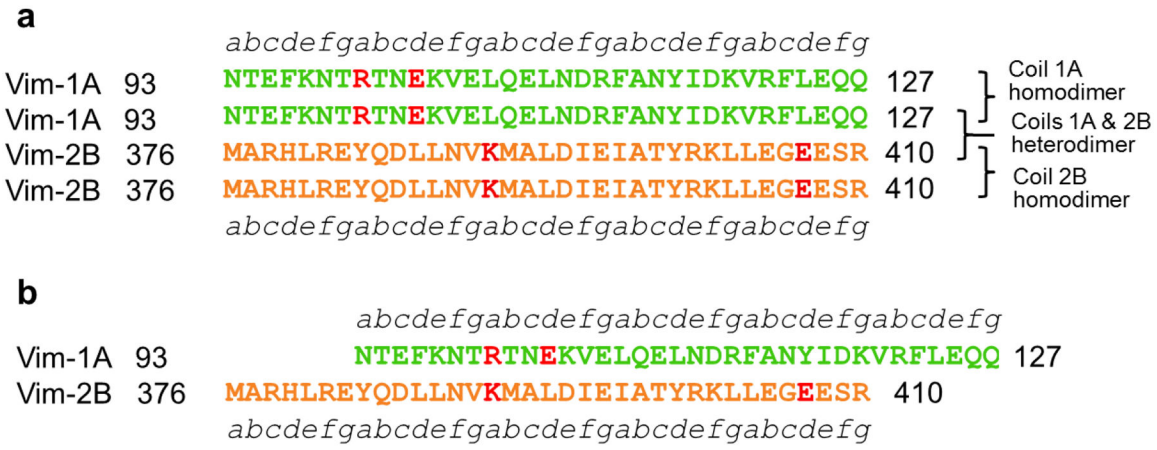

Fig. 3. Sequence alignment showing the parallel heterodimeric coiled-coil interaction between the two IFCMs of vimentin.

(a) Alignment of coil 1A and coil 2B of vimentin with a three heptad repeat overlap. Destabilizing residues in the coiled-coil homodimer of 1A and 2B are colored in red. (b) Alignment of coil 1A and coil 2B of vimentin with a two heptad repeat overlap. Destabilizing residues in the coiled-coil homodimer of 1A and 2B of vimentin are colored in red. Unfavorable core residues are found in the heterodimeric coiled-coil alignment with a two heptad repeat overlap.

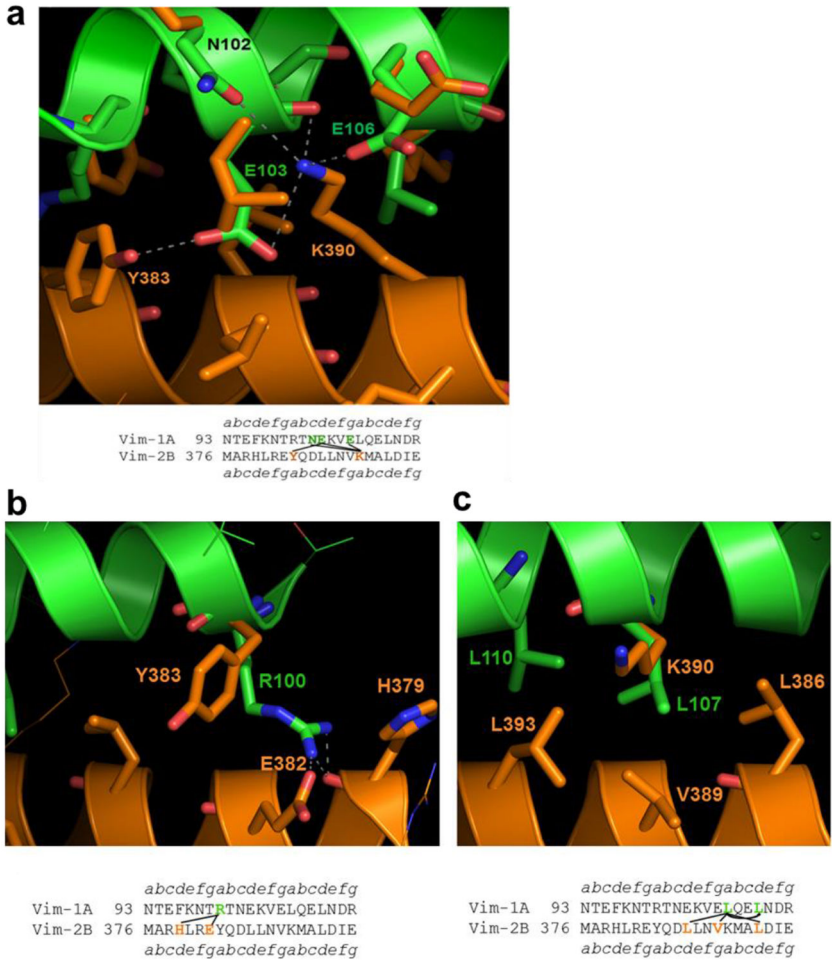

Fig. 4. Model of the parallel heterodimeric coiled coil formed in the A_{CN} interaction between the two IFCMs of vimentin with a three heptad repeat overlap.

(a) Face 1, showing coil 1A in green color superposed on the upper coil of vimentin coil 2B homodimer in orange color. In the sequence alignment below each diagram interacting residues are highlighted in bold and are connected. (b) and (c) Face 2, showing the atomic model from the other side of the coiled-coil heterodimer. The interacting residues are shown bold and connected in the sequence alignment given below each diagram.

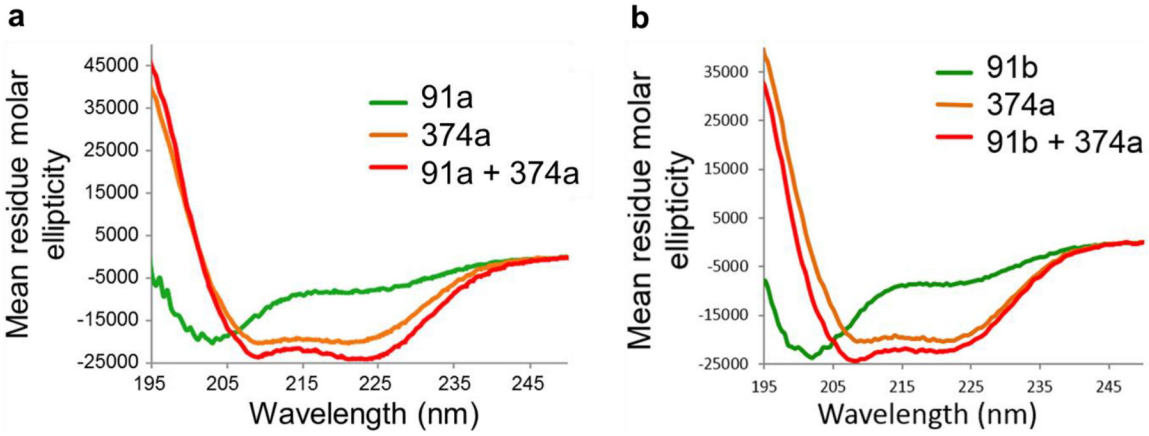

Fig. 5. CD spectra of peptides designed from the IFCMs of vimentin.

(a) CD spectra of peptide 91a (green), peptide 374a (orange), and their mixture (red). (b) CD spectra of peptide 374a (orange), peptide 91b (green), and their mixture (red). Molar ellipticity is plotted against wavelengths.

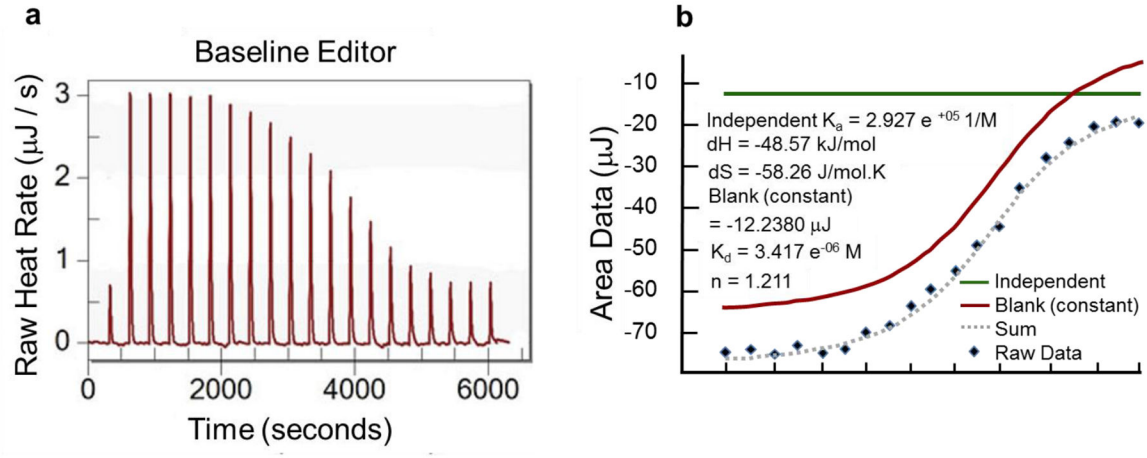

Fig. 6. ITC experiment of peptides designed from the IFCMs of vimentin.

(a) Heat released is measured in μJ/s and each peak corresponds to an injection of peptide 374a into peptide 91a. (b) The area under each injection curve is measured in μJ.

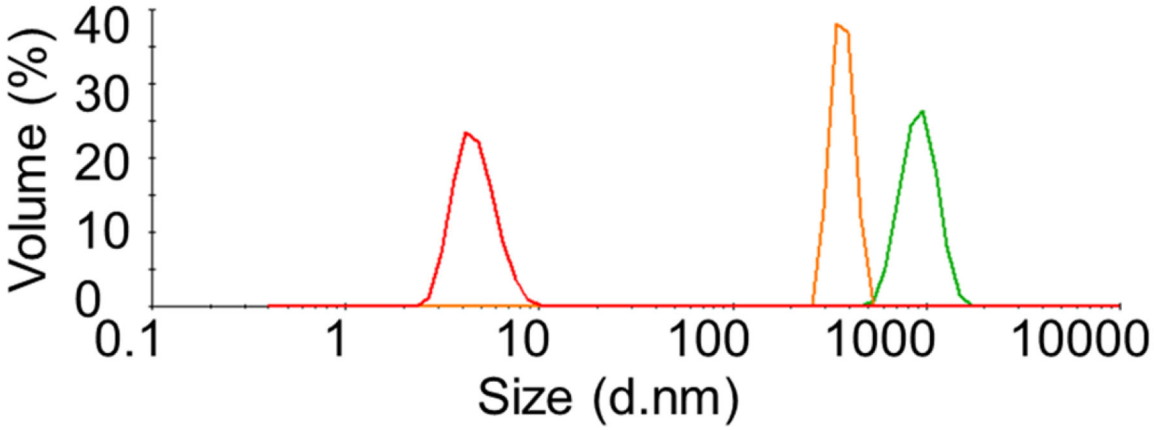

Fig. 7. DLS experiment of peptides designed from the IFCMs of vimentin.

Profiles for hydrodynamic size distribution by volume of peptide 91a (green), peptide 374a (orange) and their equimolar mixture (red) in 50mM NaCl and 10mM Tris-HCl (pH 7.5).

Scheme 1. Depiction of the head-to-tail interaction within the filament.

Coil 1 is shown in green, coil 2 is shown in orange and the IFCMs located at the ends of the central rod domain are shown in darker colors

Table 1.

Non-bonding interactions from both sides of the atomic model of A_{CN} interaction

Coil	**1A**		**2B**			
Face 1	**Residue**	**Atom**	**Residue**	**Atom**	**Distance**	**Interaction**
	Glu 106	OE1	Lys 390	NZ	2.5	Salt-bridge
	Glu 103	OE1	Tyr 383	OH	3.4	H-bond
	Glu 103	O	Lys 390	NZ	3.0	Salt-bridge
	Glu 103	OE2	Lys 390	NZ	3.5	Salt-bridge
	Asn 102	OD1	Lys 390	NZ	3.5	H-bond
Face 2	Arg 100	NH1	His 379	O	2.2	H-bond
	Arg 100	NH2	His 379	O	2.3	H-bond
	Arg 100	NH2	Glu 382	OE1	2.6	Salt-bridge
	Leu 107, Leu 110 ---- Leu 386, Val 389, Leu 393					Hydrophobic